Alexandria Engineering Journal

On blunting the crack tip through hole-drilling

Ashraf Ragab Ali Mohamed
Structural Eng. Dept., Faculty of Eng., Alexandria University, Alexandria, Egypt

This paper investigates the crack tip blunting through hole-drilling in cracked steel structures as a common practice for preventing further crack propagation due to fatigue loading or any other driving force. Fundamentals of crack blunting at the micro- and macroscopic scales have been addressed. On the micro level, it has been shown that the main idea of crack blunting is to allow for dislocation emission altering the material behavior to ductile fashion instead of the sharp crack tip cleavage which leads to brittle behavior. The issue of blunting the crack tip using a 15 mm diameter hole as per the Egyptian code has been evaluated analytically, experimentally, and numerically. Three different hole diameters of 5, 10, and 15 mm have been examined. Numerical elastic analyses showed that the diameter of the hole has a limited effect on the maximum stresses at the end of the hole and larger diameter might have a harmful effect. Numerical elastic-plastic simulations showed that plastic deformation has been achieved for all diameters considered in the analyses. Results of these simulations are in good agreement with the experiments regarding the load carrying capacity and plastic deformation. Aspects considered in this paper showed that a 5 mm diameter hole would suffice for blunting the crack tip for most practical cases.

يتناول هذا البحث موضوع تبليد أطراف الشروخ فى المنشآت المعدنية عن طريق عمل ثقوب عند أطراف الشرخ وذلك لمنع إستمرارية إمتداد الشروخ وخاصة تحت أحمال التعب. وقد تناول البحث هذا الموضوع على مستويات الميكرو والماكرو. حيث تبين أنه على مستوى الميكرو فإن عملية تبليد الشروخ تؤدى إلى تغيير سلوك المادة من القصافة إلى اللدونة مما يؤدى إلى تجنب الإنهيار المفاجئ. وقد تناول البحث تقييم لقطر الثقب المناسب حيث أن المواصفات المصرية توصى بعمل ثقب مقداره ١٥ مليمتر. وفى هذا النطاق فقد تم دراسة ثلاثة أقطار مختلفة وهى ٥ و ١٠ و ١٥ مليمتر وتم دراسة الموضوع من الناحية النظرية والعملية وكذلك عمل نماذج رياضية بإستخدام طريقة العناصر المحددة بسلوك خطى مرن وكذلك سلوك مرن – لدن. وقد أظهرت النتائج أن جميع الأقطار التي تم دراستها لها نفس التأثير فى تخفيض قيم الإجهادات وتحسين توزيعها فى المنطقة أمام الثقب. على أنه كلما زاد القطر أصبح هناك آثار جانبية غير مرغوب فيها. وقد توافقت توقعات النموذج الرياضى اللاخطى مع نتائج التجارب المعملية من ناحية الحمل الأقصى والتشكلات و أتضح من هذه الدراسة أن ثقب فتحة دائرية بقطر ٥ مليمتر كافية من الناحية العملية لتبليد أطراف الشروخ.

Keywords: Crack tip blunting, Hole-diameter, Elastic-plastic, Dislocation emission, Cleavage

1. Introduction

The presence of a crack in a steel structure or component accelerates the rate of the degradation of its load carrying capacity. The high stress and strain fields at the crack tip(s), as described by the fracture mechanics theories [1], increase the tendency of the crack to propagate especially under fatigue loading. The presence of the crack(s) in itself does not indicate failure; however, subsequent crack propagation might lead to failure. A common practice to ease the stresses near the crack tip and to prevent further crack advances is through drilling a hole at its tip(s). The process is known as blunting the crack tip. For instance, in case of crack existence in old structures, the Egyptian Code of Practice for Steel Structures [2] calls for drilling a 15 mm hole at the crack tip(s). The size of the hole as recommended by the code is rather large particularly for small cracks. The main theme of this paper is to asses the appropriateness of the hole-diameter size. This has been evaluated based on understanding the importance of crack blunting at the microscopic scale, and proposing a hypothesis followed by theoretical, experimental and numerical investigations.

2. Background

In continuum mechanics theories, the crack tip is assumed to be atomically sharp.

Crack tip blunting is one of the basic mechanisms for stopping subsequent crack propagation on different scales either accidentally or intentionally. On the microstructural level of crystalline materials, it has been shown that the bluntness of the crack tip determines the favorability of the crack propagation through cleavage or dislocation emission [3]. These two scenarios of crack advance can be depicted from fig. 1. If the energy required for the cleavage mechanism $\mathcal{G}_c$ is less than that needed for dislocation emission $\mathcal{G}_d$, the material behaves in a brittle fashion and vice versa. This has been demonstrated before by several researchers as the basic microstructural mechanisms associated with brittle versus ductile behavior (e.g., Rice and Thomson [4]). Schiotz et al. [5] have shown computationally that if the crack is blunted several atoms at the microstructure, it would be possible for the crack to emit a dislocation (ductile behavior) rather than cleavage. Fisher and Beltz [6] have demonstrated, based on microstructure finite element modeling of the blunt crack tip, that the stress field is significantly different for blunted crack tip if compared with perfectly sharp tip.

For nonmetallic materials, for instance fiber reinforced composites; the well known Cook-Gordon mechanism explained the phenomenon of crack blunting as one of the toughening mechanisms. In this case, the crack tip is blunted if it approaches a fiber through the fiber-matrix debonding. Also, the microcracking zone ahead of the crack tip in concrete and rock materials provides a type of shielding zone resulting in special type of blunting causing these materials to behave in a quasi-brittle fashion [7].

For metallic materials, Lai [8], on his paper for repairing thin aluminum pre-cracked panels, has shown experimentally that blunting the crack tip using 2 mm holes

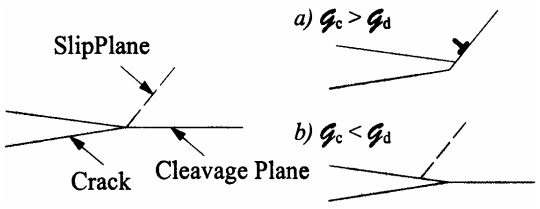

Fig. 1. Competition between a) dislocation versus b) cleavage mechanisms.

retarded the crack growth and a 50 percent increase in fatigue life of the repaired panels was achieved. Also, for those pre-cracked panels without blunting holes, no crack retardation was evident. On the other hand, Newman et al. [9] achieved a ductile behavior of blunted pre-cracked thin-sheet aluminum specimens experimentally using a 6.35 mm holes at the crack tips.

3. Plan of attack

Based on this introductory background, it is shown that crack blunting is associated mainly with the material behavior (ductile versus brittle). In materials with crystalline structure (such as steel), if the sharp crack tip is blunted several atoms, the behavior may change from brittle to ductile. If a sharp crack is to be blunted intentionally, very small hole can be drilled at its tip and the size of this hole is not that significant from the microstructural point of view. However, many other factors may play a role in this regard.

The first factor is the practical limitations on the size of the hole. With thin sheets, a 2 mm diameter hole might be appropriate as stated before [8], however, for steel plates, larger diameters are required. Questioning skilled labors regarding the minimum practical drilling hole-diameter has revealed that a 5 mm would be a lower limit, especially for relatively thick plates. The other practical limitation is related to the crack detection technique. For most practical purposes, the die-penetration technique is used, and experience has shown that crack tips are usually very sharp and quite difficult to allocate. Thus, using a very small diameter hole (e.g. 1 or 2 mm) might be impractical to be drilled exactly ahead of the crack tip.

The second factor is related to the plastic zone size in front of the crack tip resulted from the high stress and strain fields. The drilled holes should be large enough to include most of the plastic zone, thus, leaving the other parts of the material ahead of the crack tip elastic. This issue will be discussed theoretically in a following section.

The third factor is investigating if the size of the hole has a significant effect on the stress distribution ahead of the hole, and whether dislocation will emit irrespective of the hole size. This issue will be investigated both experimentally and numerically.

4. Specimens' configuration

Five basic configurations have been considered in this study; namely, SF1, SF1-A, *S*1, *S*2, and *S*3 and all specimens were 600x100x10 mm. Fig. 2 shows the specimens SF1, where a crack of 1.0 mm width has been saw-cut at the end of the specimen with 30 mm length. This type of crack does not have a sharp crack tip, rather, it was prepared in this manner to evaluate the hypothesis stated before by Schiotz et al. [5]. For the other three specimens, the same crack had been introduced but with a hole of diameter 5, 10, and 15 mm, for S1, S2, and *S*3, respectively. All the holes were drilled such that the hole boundary intersect with the crack tip. Two of each of these specimens had been tested under monotonic remote tensile stress till failure. On the other hand, the specimen SF1-A, was an analysis specimen with an edge crack length of 30 mm and with perfectly sharp crack tip.

5. Material properties

Experimental testing on tension specimens of the same material as that of the previously mentioned specimens had revealed a yield stress σ_{ys} of 288, 292, and 303 MPa with an average value of 294 MPa. The material ultimate strength σ_u were 412, 394, and 422 MPa, with an average value of 409 MPa. The percent elongation ε_u of the three specimens was 26, 21, and 22 % with an average value of 23%. These material properties will be used throughout this study.

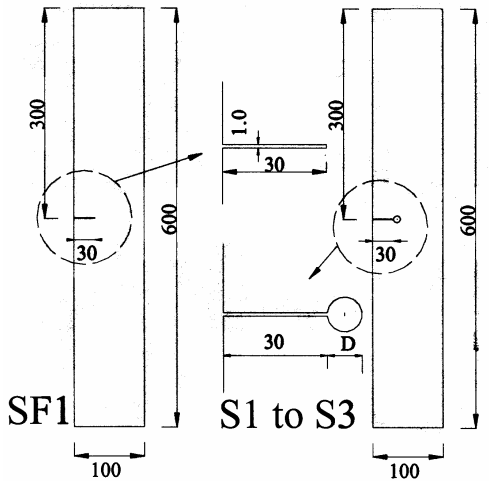

Fig. 2. Configuration for SF1 and S1 to S3.

6. Plastic zone size

The plastic zone size ahead of the crack tip is of crucial importance in this study as it is hypothesized that the hole should be drilled to remove most of this zone. This will leave the rest of the material in elastic state and eliminate any predefined slip planes of dislocation. It can be shown, based on fracture mechanics theories, [1] and by considering the von Mises yielding criteria that the size of the plastic zone r_p (the outer bound of the plastic zone) can be expressed for plane strain ($pl-\varepsilon$) and plane stress ($pl-\sigma$) conditions as:

For $pl-\varepsilon$,

$$r_p = \frac{1}{4\pi}\left(\frac{K_I}{\sigma_{ys}}\right)^2 [1.5\sin^2\theta + (1-2\nu)^2(1+\cos\theta)]\,. \tag{1-a}$$

For $pl-\sigma$,

$$r_p = \frac{1}{4\pi}\left(\frac{K_I}{\sigma_{ys}}\right)^2 [1+1.5\sin^2\theta + \cos\theta]\,. \tag{1-b}$$

Where r, θ are polar coordinates as shown in fig. 3 and K_I is the stress intensity factor for the problem in hand, which takes the general form of:

$$K_I = Q\sigma^{\infty}\sqrt{\pi a}\,. \tag{2}$$

Where Q is a geometrical function for each configuration and is tabulated elsewhere (e.g. Tada et al. [10]), σ^{∞} is the remote applied stress, and a is the crack length. By combining the two equations and rearrange, r_p can be expressed as:

Fig. 3. Plastic zone size.

For $pl-\varepsilon$,

$$\left(\frac{r_p}{aQ^2}\right)=\frac{1}{4}\left(\frac{\sigma^\infty}{\sigma_{ys}}\right)^2 [1.5\sin^2\theta+(1-2\nu)^2(1+\cos\theta)] . \quad (3\text{-a})$$

For $pl-\sigma$,

$$\left(\frac{r_p}{aQ^2}\right)=\frac{1}{4}\left(\frac{\sigma^\infty}{\sigma_{ys}}\right)^2 [1+1.5\sin^2\theta+\cos\theta] . \quad (3\text{-b})$$

Fig. 3 shows the size of the plastic zone for $\left(\sigma^\infty/\sigma_{ys}\right)$=0.5 where r_p is normalized by aQ^2. As known, the plastic zone size for the $pl-\sigma$ condition is larger than the $pl-\varepsilon$ condition. For the case of $pl-\sigma$, i.e. the plastic zone is maximum, (r_p/aQ^2) is about 0.167 at an angle of 71°. For small cracks in relatively large structures, which is valid for most of the cases, it can be shown that the geometric function Q approaches 1.0. Furthermore, in regularly inspected structures, cracks are detected, even with naked eye, with a length ranging from 10 to 20 mm. These simplified assumptions lead to a plastic zone size in the order of 1.7 to 3.3 mm, hence, a 5 mm hole-diameter would suffice to remove most of the plastically deformed parts ahead of the crack tip. If the configuration and remote stress are well defined, i.e. a, σ^∞, Q are known, a better estimate for plastic zone size can be obtained. It should be mentioned that the previous

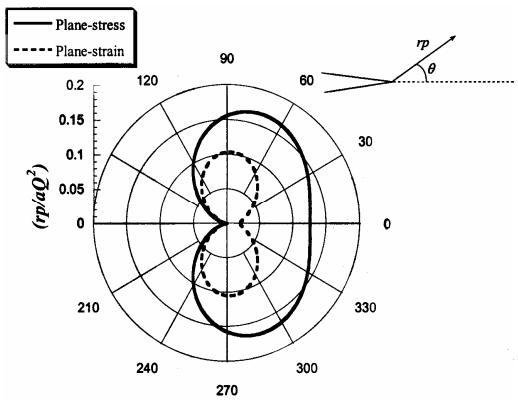

formulae are approximate; however, they provide a realistic evaluation of the plastic zone size.

7. Experimental study

The three specimens *S*1, *S*2, and *S*3 as described before were subjected to monotonic uniform remote stress at their ends till the ultimate load. A universal testing machine 1000 KN capacity was used as shown in fig. 4. Two specimens of each configuration were tested and the ultimate remote stress, the corresponding Crack Mouth Opening Displacement (CMOD), and the Hole Root Displacement (HRD) at the ultimate load for the three specimens are given in table 1. Due to the very high plastic deformation at the ultimate load, both CMOD and HRD are measured using a vernier of 0.01 mm sensitivity. The definitions of both CMOD and HDR are shown in fig. 5-a. By comparing the two specimens of each category, very close results were obtained for the ultimate load, and relatively larger differences were recorded for the deformations. The three specimens have shown considerable plastic deformation ahead of the hole as shown in fig. 5-b, c, and d. Thus, the diameter of the hole, in the range considered in this paper, had a limited effect on the dislocation emission. However, larger diameters had lower load carrying capacity due to the reduction in the ligament length.

With respect to the specimen SF1, where the crack tip was not sharp, but was blunted 1.0 mm through saw-cutting, it behaved in a brittle fashion. A crack started from one of the blunted tip corners and propagated as shown in fig. 5-e. This type of failure may be attributed to some imperfection in the blunted tip as it was prepared through saw-cutting. This observation is vital as it has two folds. The first is that it is difficult to justify the hypothesis of several-atoms blunting as proposed by Schiotz et al. [5] as imperfection might dominate the behavior. The other fold is that it is better to have a rounded blunting as this eliminates the possibility of imperfection, and the size of the blunting hole should be relatively large (in the order of 5 mm).

Another crucial observation can be depicted from fig. 5-f. This S3 specimen was loaded beyond the ultimate load, and this loading resulted in the formation of a new crack started at the end of the hole. Thus, it should be clear that blunting the crack tip is not a method of repair for cracked steel structures. Rather, it is a practice to prevent further crack propagation until repairing or replacing the cracked part. This also shows that as the stress concentration at the end of the blunting hole is relatively high, as will be shown later in analysis section, it represents a high potential for further crack formation.

Table 1
Results of the experimental work

Specimen	Ultimate stress MPa			Corresponding CMOD mm			Corresponding HRD mm		
	sample1	sample2	average	sample1	sample2	average	sample1	sample2	average
S1	219	211	215	19.35	17.85	18.60	14.10	12.20	13.15
S2	234	232	233	18.10	16.45	17.28	13.35	12.70	13.03
S3	248	244	246	15.35	14.10	14.73	11.20	10.70	10.95

Fig. 4. Test set-up.

8. Numerical analysis

Both linear elastic and elastic-plastic analyses were conducted for the configurations in fig. 2. A specialized nonlinear finite element package was used throughout (FRANC2D/L) [11]. The four specimens SF1-A, S1, S2, and S3 have been modeled through the Finite Element Method

(FEM). Eight and six-noded elements with quadratic shape functions were implemented where the eight-noded elements are used for most of the regions, and the six-noded triangular element for the transition in between. Details of element formulation are available elsewhere [12]. A very fine mesh has

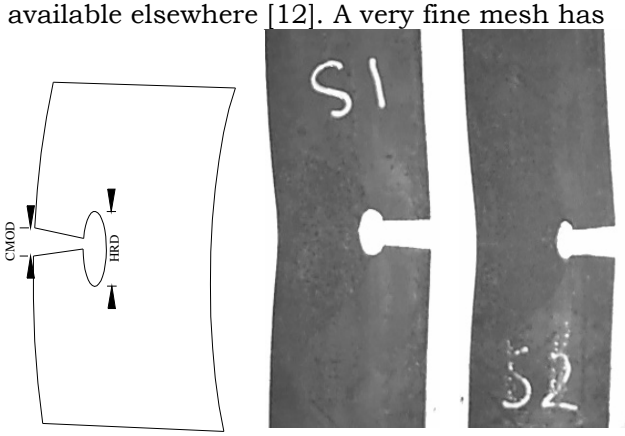

a) Definition of CMOD and HRD b) S1 at ultimate load c) S2 at ultimate load

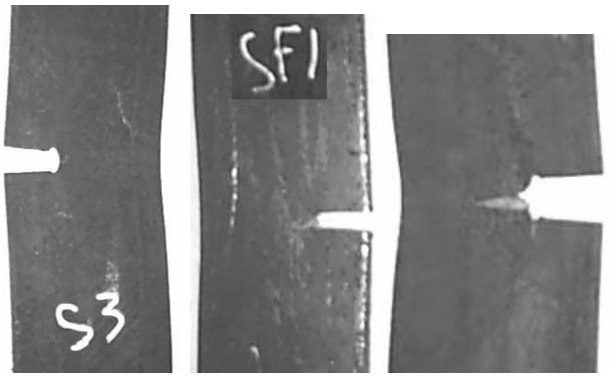

d) S3 at ultimate load e) SF1 with crack initiation f) S3 loaded beyond ultimate load

Fig. 5. Deformation and cracking for tested specimens.

been utilized around the area of interest (the hole or the crack tip) and a relatively courser mesh far from the hole. Example for the FEM mesh for S1 is shown as mesh1 (2579 nodes and 852 elements) in fig. 6. Due to the very high stress and strain gradients around the crack tip or the hole, it is critical to check whether the FEM mesh is fine enough to capture these gradients. Thus, a much finer mesh, designated as mesh2 (6017 nodes and 2000 elements) in fig. 6 was constructed. The material properties for the linear elastic material were an elastic modulus (E) of 200 GPa, and Poisson's ratio (υ) of 0.3. Comparison between the vertical elastic stress (σ_{yy}) distributions along the ligament length (Lo) due to remote working stress of 147 MPa for the two meshes is shown in fig. 7. The two responses are identical and the difference between the maximum stresses (i.e. at x/Lo=0) for the two meshes is only 0.4%. Thus, it was decided to use mesh1 throughout, especially for elastic-plastic analysis which is computationally intensive.

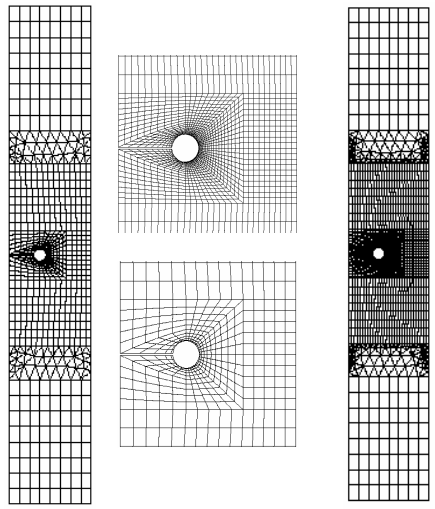

Mesh1 Mesh2 (Finer)

Fig. 6. FEM meshes for mesh fineness check.

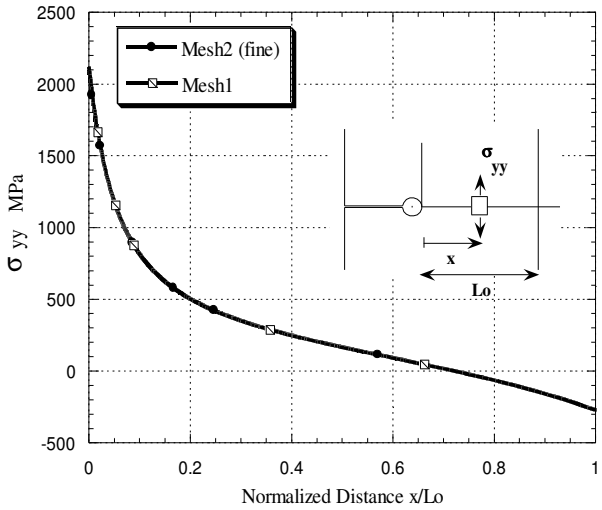

Fig. 7. Effect of FEM mesh fineness.

8.1. Elastic analysis

The focus of the linear elastic stress analysis is to evaluate if the hole size affects the stress magnitude and distribution along the ligament. The remote stress used in this analysis was a working stress of 147 MPa (i.e. $\sigma_{ys}/2$). Results of the analyses (σ_{yy} *vs. x/Lo*) for specimens S1 to S3 are plotted in fig. 8 together with the response of SF1-A. As can be depicted from the figure, increasing the hole-diameter will reduce the high stress gradient close to the hole, resulting in a better distribution of stresses. Also, the three hole-diameters reduced the maximum stress significantly as given in table 2 if compared to the sharp crack tip stress of SF1-A. However, the difference between the different hole-diameters is not significant. It should be noted that these stress values are theoretical stresses and this type of analysis was conducted mainly to compare the stress concentration for different cases. More realistic results will be shown in the elastic-plastic analysis. Also given in table 2 are the values of the Crack Mouth Opening Displacement (CMOD) for the four specimens at the working stress of 147 MPa. Increasing the hole diameter resulted in higher CMOD values leading to more compliant specimen. Furthermore, increasing the diameter of the hole will reduce the ligament length and hence increasing the load eccentricity. This has resulted in the development of compressive stresses at the end of the ligament and the magnitude of stresses and length of the compressive stress zone increase as the hole-diameter increases as depicted from fig. 8. Thus, elastic analyses revealed that drilling a hole at the crack tip will ease the stresses but increasing the hole diameter might have other harmful effects.

Table 2
Results of linear elastic analysis ($\sigma^{\circ} = \sigma_{ys}/2.0$)

Specimen	$\sigma_{yy\ max}$ MPa (at x/Lo=0)	Corresponding CMOD mm
SF1-A	7616	0.2068
S1	2082	0.5856
S2	2068	0.4127
S3	2311	0.2931

8.2. Elastic-plastic analysis

Elastic-plastic analyses have been conducted for the specimens S1 to S3 using the FEM meshes as in the elastic analysis. The constitutive model for the material behavior is shown in fig. 9. The values of σ_{ys}, σ_u, and ε_u were experimentally obtained, the other values were computed such that strain at the end of yielding zone (ε_{st}) = 10 ε_y and the strain hardening curve follows a parabola with an initial tangent modulus E_{st} =2500 MPa with a horizontal tangent at ultimate stress. Similar models have been used before in the literature [13].

An incremental displacement control procedure has been utilized with an increment size of 0.04 mm, tolerance of 0.1%, and von Mises yielding criterion were used throughout. The predicted remote stress-edge deformation curves for the three specimens are shown in fig.10 together with the average experimentally obtained load levels. Generally, larger hole-diameters resulted in lower load-carrying capacity as the ligament length decreases. Further, as given in table 3, good agreement was observed between predicted and experimental results for the three specimens with a difference in the ultimate load of 4.8, 4.3, and 5.93 % for S1, S2, and S3, respectively. The same agreement was found for the deformation at the ultimate load except for the specimen S3, where very high differences where found between numerical simulation and experimental work. The other critical aspect is that there was dislocation emission for the specimens due to the different hole-diameters indicating ductile behavior. Fig. 11 shows the contour of effective (von Mises) stresses as predicted by the elastic-plastic analysis at the end step. It is clear that there exist considerable plastic stresses in the ligament ahead of the hole for the three specimens. The shape of the plastic stress zone matches those shown before for the experimental testing in fig 5-b to d. Also, the deformed shapes of the three specimens at the end of the simulations are shown in fig. 12 which also agree with the experimental work. Elastic-plastic analysis failed to predict the cleavage mechanism observed in the

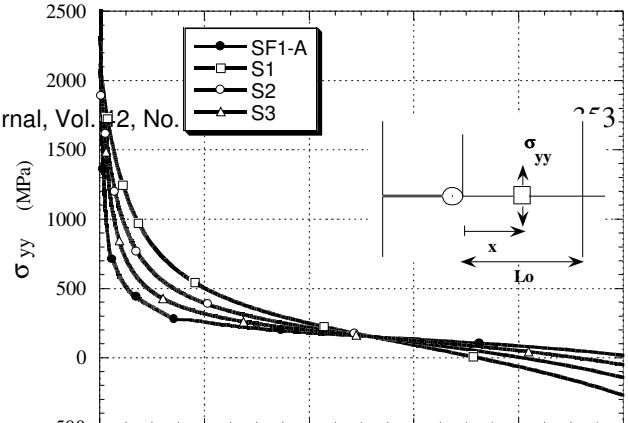

Fig. 8. Vertical Stress Component σ_{yy} along the ligament.

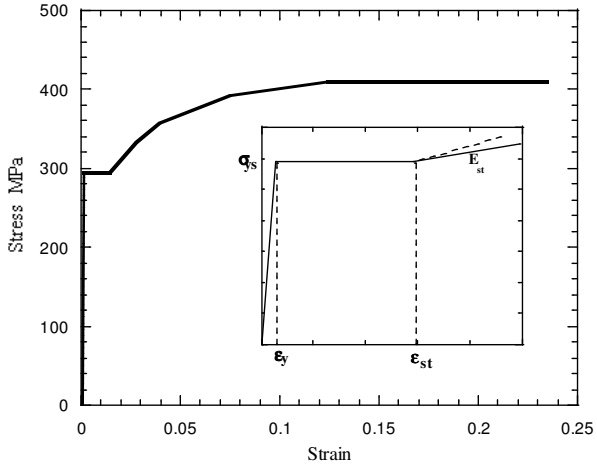

Fig. 9. Material constitutive relation used in elastic-plastic analysis.

experimental testing of SF1 as shown before in fig 5-e. This may be attributed to the factors discussed before which were not modeled in the analysis such as imperfection.

9. Conclusions

Based on the theoretical, experimental, and numerical analysis in this paper, the following conclusions can be drawn. All conclusions are limited to the sizes of the holes and material properties considered in this study:

1. Blunting the crack tip is vital for changing the material behavior to ductile, i.e. dislocation emission, instead of brittle behavior associated with cleavage.
2. Blunting the crack tip eases the stress field near the tip and results in better stress distribution. The size of the hole, is the range considered in this study, is not significant in this regard.
3. As the size of the hole for crack tip blunting increases, the load carrying capacity decreases and the specimens become more compliant.
4. Very good agreement has been found between the experimental and numerically predicted response with respect to load level, deformation, and dislocation emission.
5. A 5 mm hole-diameter would suffice in most practical cases for blunting the crack tip and plastic behavior has been achieved irrespective of the hole-diameter.

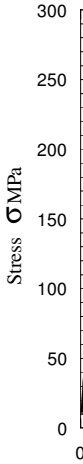

Fig. 10. Prediction of remote stress-deformation response for S1, S2, and S3.

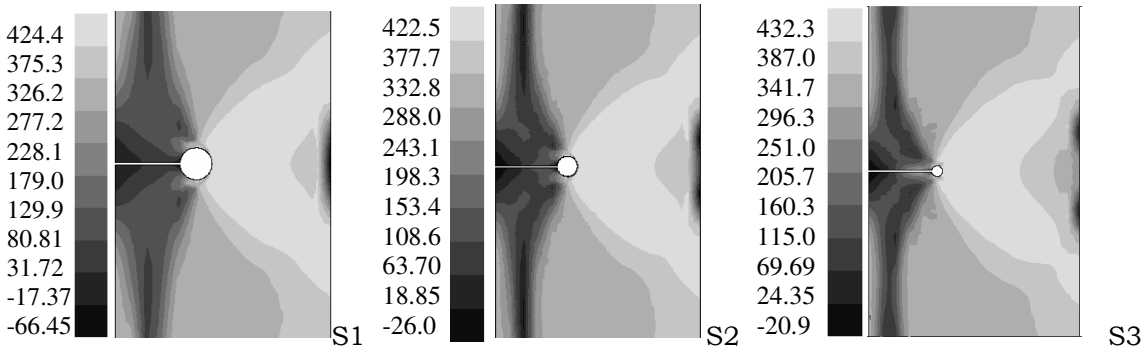

Fig. 11. Effective von Mises stresses at the end of simulation.

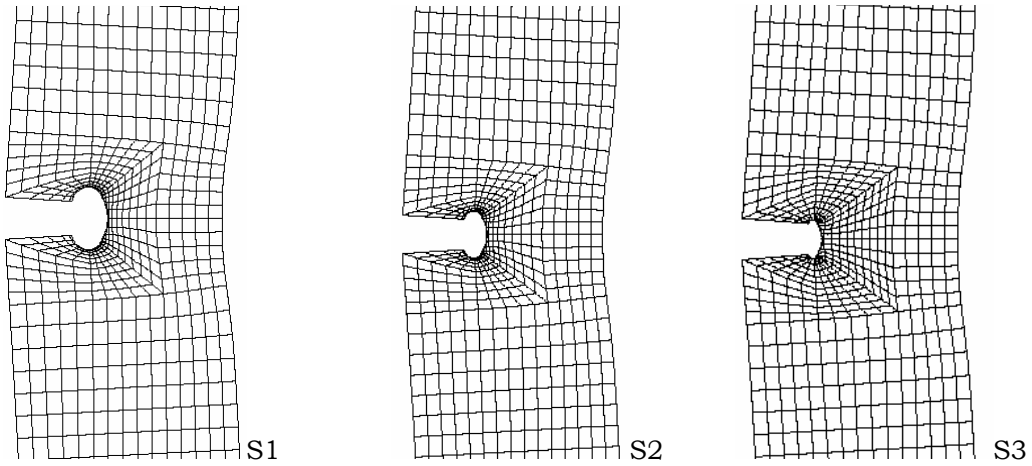

Fig. 12. Deformed shape at the end of simulation.

Table 3
Comparison between experimental results and numerical simulations

Specimen	Ultimate stress MPa			Corresponding CMOD mm			Corresponding HRD mm		
	Exp.	Num.	Diff.%	Exp.	Num.	Diff.%	Exp.	Num.	Diff.%
S1	215	225.49	4.9	18.60	17.95	-3.5	13.15	13.23	0.6
S2	233	243.01	4.3	17.28	17.77	2.8	13.03	12.97	-0.5
S3	246	260.60	5.9	14.73	16.53	12.2	10.95	11.94	9.1

References

[1] D. Broek, "Elementary Engineering Fracture Mechanics," 4th edition, Kluwer Academic Press, Boston (1991).

[2] "Egyptian Code of Practice for Steel Construction and Bridges," Minsterial Decree No. 185-1998, ARE, Ministry of Housing, Utilities, and Urban Communities, article 11.2.2.10 (2001).

[3] G. Beltz, D. Lipkin, and L. Fischer, "Role of Crack Blunting in Ductile Versus Brittle Response of Crystalline Materials," Physical Review Letters, Vol. 82 (22), pp. 4468-4471 (1999).

[4] J. Rice, and R. Thomson, "Ductile versus Brittle Behavior of Crystals," Phil. Mag. Vol. 29 (73) (1974).

[5] J. Schiolz, A. Carlsson, L. Canel, and R. Thomson, "Effect of Crack Blunting on Subsequent Crack Propagation," Mater. Res. Soc. Symp. Proc. 409 (1995).

[6] L. Fisher, and G. Beltz, "Continuum Mechanics of Crack Blunting on Atomic

Scale: Elastic Solutions," in Modelling Simulation Mater. Sci. Eng. 5, pp. 517-537 (1997).

[7] Z. P. Bazant "Size Effect in Nlunt Fracture: Concrete, Rock, Metal," Journal of ASCE, Vol. 110 Engineering Mechanics, Vol. 4, pp. 518-535 (1984).

[8] M. Lai, "Fatigue Performance of Repaired Aluminum," International Journal of Damage Mechanics, Vol. 2 (2), pp. 199-204 (1993).

[9] J. Newman, D. Dawicke, and C. Bigelow, "Finite-Element Analyses and Fracture Simulation in Thin-Sheet Aluminum Alloy," Presented at the International Workshop on Structural Integrity of Aging Airplanes, Atlanta, GA, 31 Mar.- 2 Apr. (1992).

[10] H. Tada, P. Paris, and G. Irwin, "The Stress Analysis of Cracks Handbook," Del Research Corporation (1973).

[11] D. Swenson, and M. James, "RANC2D/L: A Crack Propagation Simulator for Plane Layered Structures," Kansas State University, Manhattan, Kansas (1992).

[12] N. Ottosen and H. Petersson, Introduction to the Finite Element Method, Prentice Hall International (UK) Ltd (1992).

[13] C. Salmon, and J. Johnson, Steel Structures: Design and Behavior, 3rd Ed., Harper Collins Publishers (1990).

Received April 4, 2003
Accepted May 17, 2003